

**MODIS Observed
increase in
Greenland sediment
plumes**

B. Hudson et al.

MODIS observed increase in duration and spatial extent of sediment plumes in Greenland fjords

B. Hudson^{1,2}, **I. Overeem**², **D. McGrath**^{3,4}, **J. P. M. Syvitski**^{1,2}, **A. Mikkelsen**⁵, and **B. Hasholt**⁵

¹University of Colorado, Department of Geological Sciences, Boulder, CO, USA

²University of Colorado, Community Surface Dynamics Modeling System, INSTAAR, Boulder, CO, USA

³University of Colorado, CIRES, Boulder, CO, USA

⁴USGS Alaska Science Center, Anchorage, AK, USA

⁵University of Copenhagen, Copenhagen, Denmark

Received: 7 November 2013 – Accepted: 15 November 2013 – Published: 20 December 2013

Correspondence to: B. Hudson (benjamin.hudson@colorado.edu)

Published by Copernicus Publications on behalf of the European Geosciences Union.

Title Page

Abstract

Introduction

Conclusions

References

Tables

Figures

⏪

⏩

◀

▶

Back

Close

Full Screen / Esc

Printer-friendly Version

Interactive Discussion

Abstract

We test the hypothesis that increased meltwater runoff from the Greenland Ice Sheet (GrIS) has elevated the suspended sediment concentration (SSC) of six river plumes in three fjords in southwest Greenland. A SSC retrieval algorithm was developed using the largest in situ SSC dataset for Greenland known and applied to all cloud free NASA Moderate Resolution Imaging Spectrometer (MODIS) reflectance values in the Terra image archive (2000 to 2012).

Melt-season mean plume SSC has not increased as anticipated, with the exception of one river. However, positive statistically significant trends involving metrics that described the duration and the spatial extent of river plumes were observed in many locations. Zones of sediment concentration $> 50 \text{ mg L}^{-1}$ expanded in three river plumes, with potential consequences for biological productivity. The high SSC cores of river plumes ($> 250 \text{ mg L}^{-1}$) expanded in one-third of study locations. When data from study rivers was aggregated, higher volumes of runoff were associated with higher melt-season mean plume SSC values, but this relationship did not hold for individual rivers. High spatial variability between proximal plumes highlights the complex processes operating in Greenland's glacio-fluvial-fjord systems.

1 Introduction

The Greenland Ice Sheet (GrIS) is the largest landbound ice mass in the Northern Hemisphere (Serreze and Barry, 2005). It stores the equivalent of 7 m of global sea level (Bamber et al., 2013). Freshwater discharge from the GrIS is an important contributor to the Arctic hydrological cycle (Mernild et al., 2011), though few multi-year runoff observations exist (Cowton et al., 2012; Hasholt et al., 2013; Rennermalm et al., 2013).

The GrIS has lost approximately $142 \pm 49 \text{ Gtyr}^{-1}$ of mass between 1992 and 2011 (Shepherd et al., 2012) or $\sim 0.005\%$ of its total mass per year assuming a volume of

TCD

7, 6101–6141, 2013

MODIS Observed increase in Greenland sediment plumes

B. Hudson et al.

Title Page

Abstract

Introduction

Conclusions

References

Tables

Figures

◀

▶

◀

▶

Back

Close

Full Screen / Esc

Printer-friendly Version

Interactive Discussion

positive degree-days, was the most significant driver of regional suspended sediment concentration variability in fjords.

We hypothesize that *increased freshwater discharge due to increased ice sheet melt has elevated the melt-season suspended sediment concentration of Greenlandic fjords*. While we recognize that the suspended sediment concentration (SSC) of Greenland's fjords are an understudied problem, it offers the potential to be an important indicator of environmental change. The sediment exported by a glacier is a function of the efficiency of its subglacial drainage network, its sediment production rate, and its sediment storage ability (Fausto et al., 2012).

Fjord SSC is not only diagnostic of subglacial sediment dynamics but also of fjord health. Suspended sediment impacts the availability of light (Retamal et al., 2008). High levels of SSC in fjords may impact biological productivity, such as pelagic zooplankton feeding efficiency and production rates (Arendt et al., 2011). However, sediment delivers nutrients to the coastal ocean at the same time (Statham et al., 2008).

Widespread in situ observations of SSC in Greenland are logistically infeasible; in fact Hasholt (1996) and Hasholt et al. (2006) identified < 15 locations where sediment dynamics had been studied, even for a short period of time. Instead, recent efforts have focused on using orbital remote sensing to monitor GrIS sediment dynamics (Chu et al., 2009, 2012; McGrath et al., 2010; Tedstone and Arnold, 2012). A goal of this paper is to provide an improved SSC retrieval algorithm, based on in situ observations, for future investigations and to better characterize the variability of SSC in fjords in southwest Greenland.

2 Study areas and approach

Six proglacial river systems draining into three major fjords in southwest Greenland were selected: Pakitsuup, Kangerlussuaq, and Ameralik fjords (Fig. 1). To determine the portions of the GrIS that contribute melt to each river we calculated the local hydrostatic pressure field of the ice sheet, which combines surface elevation data with

TCD

7, 6101–6141, 2013

MODIS Observed increase in Greenland sediment plumes

B. Hudson et al.

Title Page

Abstract

Introduction

Conclusions

References

Tables

Figures

⏪

⏩

◀

▶

Back

Close

Full Screen / Esc

Printer-friendly Version

Interactive Discussion



MODIS Observed increase in Greenland sediment plumes

B. Hudson et al.

Title Page

Abstract

Introduction

Conclusions

References

Tables

Figures

⏪

⏩

◀

▶

Back

Close

Full Screen / Esc

Printer-friendly Version

Interactive Discussion

basal topography (Lewis and Smith, 2009; Cuffey and Patterson, 2010). We used surface elevation of the Greenland Mapping Project (GIMP) digital elevation model (Howat et al., 2013) and the University of Kansas Center for the Remote Sensing of Ice Sheets (CRESIS) Jacobshavn composite dataset for the Pakitsuup region (https://data.cresis.ku.edu/data/grids/) and the coarser basal topography from Bamber et al. (2001) for the Kangerlussuaq and Ameralik regions. Flow routing and catchment delineation was performed following a D-infinity approach using RiverTools 3.0 (Peckham, 2009). Catchment areas describe only the portion of the watershed covered by glacial ice, as these areas are the major sources of water and sediment to the systems studied.

2.1 Pakitsuup Fjord

Pakitsuup Fjord (also spelled Pakitsoq) is located near the town of Ilulissat, and receives melt from two small river systems. The “Pakitsuup North” River (69°31′45.5″ N, 50°13′23.7″ W) has two branches, respectively 8 and 10 km long. It drains a catchment of the GrIS $\sim 302 \text{ km}^2$ (Table 1), which reaches a maximum height of ~ 1169 meters above sea level (m.a.s.l.). The “Pakitsuup South” River (69°26′5.9″ N, 50°27′53.3″ W) flows 7 km from the margin of the GrIS that feeds it along its southern tributary. A northern tributary flows 20 km through a series of lakes, before combining with the southern tributary approximately 4 km from the river mouth. It is the smallest catchment studied ($\sim 143 \text{ km}^2$) with the lowest maximum elevation (~ 1020 m.a.s.l.). Mernild et al. (2010) estimate that the equilibrium line altitude (ELA) for the region is approximately 1125 m.a.s.l.

2.2 Kangerlussuaq Fjord

Three major river systems discharge water and sediment into Kangerlussuaq Fjord (Søndre Strømfjord).

Kangaussarssup Sermia (“KS” on Fig. 1), discharges water to the river uninterrupted by lakes. On the north side of Kangaussarssup Sermia two ice margin lakes exist. These lakes historically drained down a valley (the Austmannadalen) to a point approximately 7 km from the river mouth. Since 2004, the lakes drain north into Kangiata Nunaata Sermia (“KNS” on Fig. 1, Weidick and Citterio, 2011). As the MODIS record straddles this drainage realignment, Table 1 provides two delineations, one with the lakes (Naujat Kuat) and one without (Naujat Kuat – Small). At its smallest, the on-ice catchment area is 356 km². This uncertainty in drainage basin delineation does not affect the maximum elevation of the drainage or the general shape of the hypsometric curve.

3 Methods

3.1 Suspended sediment samples

We collected surface water samples as part of our oceanographic surveys in the three fjords during the 2008, 2010, 2011, and 2012 summer seasons (Table 2). In total, one hundred and forty three samples were utilized for ground-truthing work, which collectively covered 12 days in all major melt months. The SSC retrieval algorithm dataset also contained three additional water samples collected from Orpigsoq Fjord (68°38′30.9″ N, 50°54′45.5″ W) on 2 July 2011 though this paper did not analyze that fjord.

As Fig. 1 shows, sampling followed variably spaced transects. Water samples were collected by dipping a 1000 mL bottle into the surface layer while a handheld GPS noted the location. Samples were then vacuum filtered through pre-weighed Whatman GF/F filters, rinsed with distilled water to remove salt, freeze dried, and re-weighed to determine SSC. Suspended sediment concentrations ranged between 1.2 and 716 mgL⁻¹ with a mean SSC of 73 mgL⁻¹. One sample collected from the shallow river mouth of the Watson river on 9 July 2011 had an SSC of 1581 mgL⁻¹ but was excluded from

TCD

7, 6101–6141, 2013

MODIS Observed increase in Greenland sediment plumes

B. Hudson et al.

Title Page

Abstract

Introduction

Conclusions

References

Tables

Figures

⏪

⏩

◀

▶

Back

Close

Full Screen / Esc

Printer-friendly Version

Interactive Discussion

analysis because it could not be determined if the sampling boat had disturbed bottom sediments.

3.2 SSC retrieval algorithm based on MODIS reflectance

MODIS Terra MOD02 250 m imagery and the MOD03 geolocation data product for each swath image were downloaded from NASA's Reverb Earth Science Data Discovery Tool (<http://reverb.echo.nasa.gov/reverb/>). Exelis ENVI 4.8 software, including the MODIS Conversion Toolkit (<http://www.exelisvis.com>) georeferenced, bow tie, and atmospherically corrected imagery (using dark object subtraction). Each scene covered a geographic area that included cloud-free open ocean pixels required for accurate dark object subtraction. (Kirk, 2011; Miller and McKee, 2004). A Danish National Survey and Cadastre (DNSC) Greenland coastline vector file confirmed the geospatial accuracy of each image. If needed, MODIS imagery was manually shifted to agree with the DNSC coastline.

SSC values were compared to co-located band one (620 to 670 nm) and two (841 to 876 nm) reflectance values. Barbieri et al. (1997) defined the MOD02 reflectance data product as the bidirectional reflectance factor of the Earth (ρ_{ev}) multiplied by cosine of the solar zenith angle at the earth scene (θ_{ev})

$$\rho_{ev} \times \cos \theta_{ev} \cdot \quad (1)$$

With ρ_{ev} defined as

$$\rho_{ev} = \frac{L_{ev}}{E_i \cos \theta_{ev}}, \quad (2)$$

where L_{ev} is the earth view spectral radiance ($\text{W m}^{-2} \text{sr}^{-1} \mu\text{m}^{-1}$), and E_i is solar irradiance ($\text{W m}^{-2} \mu\text{m}^{-1}$). Combing these two equations, reflectance is calculated as

$$R_{rs} = \frac{L_{ev}}{E_i}. \quad (3)$$

MODIS Observed increase in Greenland sediment plumes

B. Hudson et al.

Title Page

Abstract

Introduction

Conclusions

References

Tables

Figures

◀

▶

◀

▶

Back

Close

Full Screen / Esc

Printer-friendly Version

Interactive Discussion



Ocean color remote sensing literature often define R_{rs} as radiance reflectance (Kirk, 2011) or remote sensing reflectance (Mobley, 1999), though technically E_i should be downwelling irradiance directly above the surface of the water (E_d), not from the top of atmosphere (E_i). Despite this difference, we use the R_{rs} notation. Following Miller and

5 McKee (2004), variations in scene solar zenith angle were corrected on an individual pixel basis to arrive at

$$R_{rsc} = R_{rs} \times \frac{1}{\cos \theta_{ev}}. \quad (4)$$

We develop a SSC retrieval algorithm using both MODIS band one and two and the co-located in situ sediment samples (Fig. 2). Unlike previous MODIS algorithms which became saturated above 80 mgL^{-1} (e.g. Chu et al., 2009), the addition of band two, which measures reflectance in the near infrared, remains sensitive to higher sediment concentrations. The final retrieval algorithm used was

$$SSC = 1.80 \times \exp(19.11 \times (R_{rsc,B1} + R_{rsc,B2})). \quad (5)$$

The retrieval dataset included samples from four different fjords with variable salinity regimes. Using a Seabird 19 conductivity, temperature, and depth probe, we measured salinities as high as 25 PSU (Ameralik Fjord) and as low as 1 PSU (Kangerlussuaq Fjord) in the top meter of the surface layer where samples were taken. The variable salinity during our oceanographic surveys, and the independence of the relationship on this parameter, suggests that this retrieval technique can be applied to disparate locations with variable oceanographic conditions.

20 Following algorithm development, we processed ~ 300 sea ice-free swath scenes per year (spanning day of the year 135 to 295) to map fjord SSC values over the entire melt season. Appendix A describes the full processing details.

MODIS Observed increase in Greenland sediment plumes

B. Hudson et al.

Title Page

Abstract

Introduction

Conclusions

References

Tables

Figures

⏪

⏩

◀

▶

Back

Close

Full Screen / Esc

Printer-friendly Version

Interactive Discussion



3.3 Error from sampling irregularities caused by clouds

Since the year 2000, MODIS Terra satellite observations provide an ongoing daily record in this region, although, as common in polar regions, the presence of clouds compromise the imagery's utility as an observational tool. In total, clear-sky existed for between 5 and 21 % of all available fjord pixels in a given summer season.

Computational experiments following Gregg and Casey (2007) assessed this sampling bias. A "truth" dataset based on the entire 13yr data record was created and then masked with MODIS observed cloud cover to understand how cloud obscuration impacted SSC statistics.

To create the "truth" dataset we calculated the 13yr mean SSC map on a pixel-by-pixel basis as

$$13 \text{ year SSC} = \frac{\sum_{\text{year}=2000}^{2012} \sum_{\text{day}=135}^{295} \text{SSC}_{i,j}}{\sum_{\text{year}=2000}^{2012} N_{i,j}}. \quad (6)$$

Where N was the number of times the pixel passed all tests and was used in the analysis, i is pixel location in the horizontal direction, and j is pixel location in the vertical direction. The cloud masking scheme set SSC values to equal not-a-number if a cloud was detected, and thus excluded cloud influenced reflectance values from the statistics.

We then used the 13yr mean SSC map as a spatial template to mimic seasonal SSC fluctuations by multiplying it by a randomly perturbed sinusoidal factor, the scene intensity, I_s that peaked near day 190 of each melt-season simulation.

$$\text{SSC}_{i,j} = \overline{13 \text{ year SSC}_{i,j}} \times I_s \quad (7)$$

3.4 Selection of metrics

Three characteristic metrics were selected to describe plume dynamics and trends over the 13 yr record: melt-season mean SSC (SSC_{msm}), percent available fjord pixels in a melt season above 50 mgL^{-1} ($P_{>50}$), and above 250 mgL^{-1} ($P_{>250}$). The melt season was defined as day of the year 135 through day 295 (~ 15 May through 22 October). SSC_{msm} was selected because values were closest to “truth” values. $P_{>50}$ was selected because it matches the threshold Arendt et al. (2011) used in a recent study near Nuuk in Godthåbfjord for significant impact on copepods and secondary production. $P_{>250}$ was selected because SSC above 250 mgL^{-1} approximately maps the plume core or zone of flow establishment (Albertson et al., 1950). $P_{>50}$ and $P_{>250}$ were also the most consistent metrics between years.

SSC_{msm} deviated the least from the “truth” dataset. At most, it underestimated “truth” values by 16 % and overestimated by 38 %. On average it underestimated by 16 % and overestimated by 12 %. The maximum range of percent errors found for SSC_{msm} was 54 % (Naujat Kuat), with a mean of 36 %.

$P_{>50}$ estimates were between 67 and 91 % below “truth” values. The maximum range in the deviation from the “truth” using $P_{>50}$ for a plume was 22 % (Umiiviit), with an average range of 15 %. As Fig. 5d–f shows, $P_{>250}$ estimates were similar, between 63 and 92 % below “truth” values. The maximum range in the deviation from the “truth” was 20 % (Sarfartoq), with an average range of 16 %. Cloud obscuration prevents $P_{>t}$ metrics from correctly calculating the true number of times fjord pixels exceed a given value. Thus, absolute values reported may not be reliable. However, we argue this bias did not compromise the usefulness of the metric to detect trends.

We assigned error bars that symmetrically divided the mean range of variability found ($SSC_{msm} \pm 18\%$, $P_{>50} \pm 7.5\%$, $P_{>250} \pm 8\%$). The large bias in $P_{>t}$ values should also be remembered when interpreting results. We then added error associated with the SSC retrieval to bring overall error assigned to melt-season metrics to: $\pm 19\%$ for SSC_{msm} and $\pm 10\%$ for $P_{>t}$ metrics.

and 99 % interval for the Pakitsuup North plume ($p = 0.010$), and the Sarfartoq plume ($p = 0.006$).

4.3 Comparison of fjord SSC to river discharge and ice sheet runoff

Implicit in this paper's hypothesis was that plume SSC and discharge would be correlated, as they often are for the suspended sediment concentration of a river and its discharge. Instead, we find plume SSC_{msm} does not directly correlate to the yearly volume of water a river delivered to the ocean.

Total annual river discharge did not closely correspond to SSC_{msm} using the Watson gauge data (Hasholt et al., 2013). For example, in 2007 moderate yearly discharge ($3.5_{-0.52}^{+1.68} \text{ km}^3 \text{ yr}^{-1}$) corresponded with the highest SSC_{msm} recorded ($216 \pm 41 \text{ mg L}^{-1}$). Yet in 2011, similar or larger discharge ($3.9_{-0.56}^{+1.76} \text{ km}^3 \text{ yr}^{-1}$) produced one of the lowest SSC_{msm} values ($127 \pm 24 \text{ mg L}^{-1}$).

The poor correlation between these two variables also exists when RACMO2 annual runoff totals were used to extend the analysis in both time and to additional rivers. Of note, the Naujat Kuat plume SSC_{msm} was negatively correlated to RACMO2 runoff ($r^2 = -0.6$, $p = 0.050$).

However, when data from multiple river plumes was aggregated we found larger discharge catchments predicted by the RACMO2 model tended to have higher SSC_{msm} values (Fig. 9; $r^2 = 0.64$, $p < 0.001$, $n = 44$). This result agrees with Chu et al. (2012) that found melt (as determined from a positive degree day model) was correlated to SSC for large, spatially aggregated 100 by 100 km grid cells.

4.4 Trends between rivers

Melt-season metrics often showed similar patterns between river plumes (Tables 3 through 5). For example, all river plumes in 2009 displayed SSC_{msm} at or below 2000 to 2012 mean conditions, while during the warm 2010 year all plumes displayed SSC_{msm} at or above 2000 to 2012 mean conditions.

MODIS Observed increase in Greenland sediment plumes

B. Hudson et al.

Title Page

Abstract

Introduction

Conclusions

References

Tables

Figures

⏪

⏩

◀

▶

Back

Close

Full Screen / Esc

Printer-friendly Version

Interactive Discussion



MODIS Observed increase in Greenland sediment plumes

B. Hudson et al.

Title Page

Abstract

Introduction

Conclusions

References

Tables

Figures

⏪

⏩

◀

▶

Back

Close

Full Screen / Esc

Printer-friendly Version

Interactive Discussion

Plume conditions also varied independently between rivers. All fjords studied with multiple rivers displayed complex SSC responses in certain years, even for plumes with nearby catchments that presumably experienced similar surface melt conditions. During the extreme melt year of 2012 (Nghiem et al., 2012; McGrath et al., 2013), the Watson River plume SSC_{msm} was at or below its 2000 to 2012 mean, while the Umiiviit River plume with a catchment directly south of the Watson's, experienced a SSC_{msm} $43 \pm 17\%$ higher than its 13 yr mean. This asynchronicity is especially notable as the rivers discharge into the same fjord, and thus background oceanographic conditions (salinity and tidal conditions) are very similar. Differences in SSC for the core of the plume appear to drive this asynchronicity. Both the Watson and Umiiviit has $P_{>50}$ metrics elevated above their 13 yr mean, but Watson's $P_{>250}$ metric was close to mean conditions, while the Umiiviit was $83 \pm 19\%$ above. Figure 11d shows that the distal plume was above mean values, while pixels near the river mouth were below mean values.

River plumes displayed asynchronicity in other years. During another reportedly high melt year, 2002 (Hanna et al., 2008), the Umiiviit River plume SSC_{msm} was close to its 13 yr mean SSC, while the Watson SSC_{msm} was $28 \pm 14\%$ below its 13 yr mean SSC. In 2005, the Umiiviit plume SSC_{msm} was at or above its 13 yr mean SSC, while the Sarfartoq River SSC_{msm} , with a catchment abutting Umiiviit's GrIS catchment, was $23 \pm 15\%$ below its 13 yr mean SSC.

Observed asynchronicity is indicative of the complex sediment dynamics expected in systems controlled by glaciers. Collins (1990) hypothesized that variability in sub-glacial hydrologic networks drove variability in SSC emerging from glaciers. Stott and Grove (2001) recorded, "transient flushes" of increased SSC without increases in discharge for a glaciated (non-GrIS) catchment in Greenland. As mentioned in Sect. 1, river sediment dynamics often show a relationship between discharge and SSC. However, the variable response found may indicate in certain years that ice sheet sediment dynamics, not river sediment dynamics have been the dominant control on suspended sediment delivery to the coastal ocean.

5 Conclusions

We developed a retrieval algorithm capable of using MODIS reflectance to measure SSCs in fjords around Greenland. The SSC retrieval algorithm utilized the largest, most geographically expansive suspended sediment concentration dataset for Greenland. Data were collected over four different melt seasons between 2008 through 2012, three different melt months, and four different fjords with highly variable oceanographic conditions. Most of the geologic terrain eroded by the GrlS that drain into study fjords is similar, consisting of Archean and Paleoproterozoic age gneiss (Escher and Pulvertaft, 1995) and the geologic terrain in southwest Greenland sourcing river plumes is generally similar. As a result we argue that the retrieval algorithm is applicable to a larger area than just the study fjords.

The retrieval utilized both the red visible (band one, 620 to 670 nm) and near infrared (band two, 841 to 876 nm) 250 m resolution bands of MODIS. The combination of these bands provided accurate retrievals of SSC concentrations much higher than the 80 mgL^{-1} threshold band one can detect by using just a single band (Chu et al., 2009). In addition, a rigorous cloud detection scheme was developed for differentiating between turbid water and clouds, which minimizes cloud contamination of the retrieval.

An analysis using this retrieval on 13 yr of MODIS imagery showed that SSC_{msm} has increased for most plumes. Intra-annual and regional variability is large in Arctic regions though, and this makes it difficult to arrive at statistically significant trends over the 13 yr record.

Metrics describing the duration and the spatial extent of river plumes responded more pronouncedly. The high concentration plumes that can impair biological productivity expanded in most fjords and one-third of the river plumes expand its high concentration core zone in time and extent (95 % confidence interval).

While the relationship between the SSC_{msm} of a river plume and its volume of water discharged is not correlated inter-annually, there appears to be a relationship between

TCD

7, 6101–6141, 2013

MODIS Observed increase in Greenland sediment plumes

B. Hudson et al.

Title Page

Abstract

Introduction

Conclusions

References

Tables

Figures

⏪

⏩

◀

▶

Back

Close

Full Screen / Esc

Printer-friendly Version

Interactive Discussion

yearly modeled runoff totals and SSC_{msm} when rivers are studied in regional aggregate. We found that larger rivers tended to have higher plume SSC_{msm} .

The behavior of fjord sediment plumes over the MODIS record was complex, and variable from catchment to catchment, even in catchments that are extremely proximal to one another. This high spatial and temporal variability suggests that approaches that treat the GrIS as a whole, or even composed of distinct regions, may not be applicable to the study of sediment dynamics. Numerous and frequently non-linear processes operating in the glacio-fluvial-fjord systems preclude a simple relationship between these parameters, yet orbital remote sensing of sediment dynamics still offers a unique and important perspective for observing change in the GrIS system.

Appendix A

MODIS batch processing

Due to the high volume of MODIS swath imagery available scripts written in the Python 2.7 programming language requested, downloaded, and processed required MODIS products. Spatial subsets of MODIS MOD02, MOD03, and MOD35_L2 data for all three study fjords were requested and downloaded using the MODAPS Web Services Application Programming Interface (<http://ladsweb.nascom.nasa.gov/data/api.html>).

Multiple scientific datasets were processed to accurately extract SSC concentrations. The following steps were taken to process reflectance imagery. Only scenes imaged between 13:00 and 17:00 UTC were processed to control for solar illumination.

1. MOD02 band one and two scaled integers were converted into R_{rs} using the procedure outlined in the MODIS Level 1B Product User's Guide (Toller et al., 2009)
2. R_{rs} values were corrected for atmospheric effects using dark object subtraction by finding the lowest reflectance value in the scene and subtracting all scene reflectance values by it

MODIS Observed increase in Greenland sediment plumes

B. Hudson et al.

Title Page

Abstract

Introduction

Conclusions

References

Tables

Figures

⏪

⏩

◀

▶

Back

Close

Full Screen / Esc

Printer-friendly Version

Interactive Discussion



MODIS Observed increase in Greenland sediment plumes

B. Hudson et al.

Title Page

Abstract

Introduction

Conclusions

References

Tables

Figures

⏪

⏩

◀

▶

Back

Close

Full Screen / Esc

Printer-friendly Version

Interactive Discussion

3. R_{rs} were corrected with the MOD03 solar zenith angle product
4. Pixels that had a solar zenith angle greater than 60° were masked out
5. A land mask derived from the DNSC coastline and Landsat 7 Global Land Survey data (<http://gls.umd.edu/>) was used to mask out land pixels, and pixels that had a mixture of land and water in them to avoid land contamination effects.
6. A supplementary mask omitted all pixels wherein band two reflectance was greater than 0.17 for zones near each river mouth, and 0.13 for the rest of each fjord.

For Ameralik Fjord, all scenes between day 135 and 295 were considered. For Kangerlussuaq and Pakitsuup fjords, scenes were considered as soon as ice-free conditions were observed for each unique year. For Kangerlussuaq Fjord this ranged between day 143 and day 160. For Pakitsuup Fjord it ranged between day 144 and day 166.

The MOD35_L2 cloud mask uses many of the 36 MODIS bands to detect and mask clouds. However it incorrectly masks as clouds the highly turbid core of river plumes, due to the faulty assumption that water in the near infrared should have very low reflectance. For turbid water, the MOD35_L2 visible reflectance test (bit 20) and reflectance ratio test (bit 21) incorrectly classify turbid plumes as cloud (Ackerman et al., 2006). Instead, a custom cloud mask was built from MOD35_L2 data using the following clouds tests, and a custom mask described in Hudson et al. (2013). The following tests were applied (for more detail on tests see Ackerman et al., 2006)

1. Non-cloud obstruction (i.e. smoke from fires, dust storms) (bit 8)
2. Thin cirrus test using 1380 nm light (bit 9)
3. Shadow test for high confidence clear pixels (bit 10)
4. Thin cirrus test independent of bit 9, (bit 11)

MODIS Observed increase in Greenland sediment plumes

B. Hudson et al.

Title Page

Abstract

Introduction

Conclusions

References

Tables

Figures

⏪

⏩

◀

▶

Back

Close

Full Screen / Esc

Printer-friendly Version

Interactive Discussion

5. High cloud test using 6700 nm light (bit 15)
6. IR temperature difference test using 8600, 11 000,12 000 nm light (bit 18)
7. Low level water clouds test using difference between 11 000 nm and 3900 nm light (bit 19)
- 5 8. Test described in Hudson et al., 2013.

If any test was failed, the pixel was excluded from analysis. All datasets were then gridded to a common 250 m by 250 m UTM grid using MOD03 and MOD35_L2 geolocation data.

Acknowledgements. This project was funded through NSF-OPP Award 0909349. We thank CH2M Hill – Polar Field Services for logistic support, Michael Rosing, Jorgen Mortensen, Karsten Lings, and Silver Scivoli for help with oceanographic surveys, Aaron Zettler-Mann, Ursula Rick, Katy Barnhart, Albert Kettner, and Leif Anderson helped with field and oceanographic work. We thank Alberto Reyes (Queen’s University Belfast) for collection of samples used from Orpigsoq Fjord, Wendy Freeman for help in the processing of sediment samples, and Jonathan Bamber (University of Bristol), Janneke Ettema (University of Twente), and Michiel van den Broeke (Utrecht University) for sharing RACMO2 data.

References

- Ackerman, S., Strabala, K., Menzel, P., Frey, R., Moeller, C., Gumley, L., Baum, B., Wetzel Seeman, S., Zhang, H.: Discriminating clear-sky from clouds with MODIS, Algorithm Theoretical Basis Document (MOD35), Version 5.0, NASA, MODIS Cloud Mask Team, Madison, WI, 125 pp., 2006
- Albertson, M. L., Dai, Y. B., Jensen, R. A., and Rouse, H.: Diffusion of submerged jets, T. Am. Soc. Civ. Eng., 115, 639–664, 1950.
- Arendt, K. E., Dutz, J., Jonasdottir, S. H., Jung-Madsen, S., Mortensen, J., Moller, E. F., and Nielsen, T. G.: Effects of suspended sediments on copepods feeding in a glacial influenced sub-Arctic fjord, J. Plankton Res., 33, 1526–1537, doi:10.1093/plankt/fbr054, 2011.

MODIS Observed increase in Greenland sediment plumes

B. Hudson et al.

Title Page

Abstract

Introduction

Conclusions

References

Tables

Figures

◀

▶

◀

▶

Back

Close

Full Screen / Esc

Printer-friendly Version

Interactive Discussion

sheet revealed by high-resolution climate modeling, *Geophys. Res. Lett.*, 36, L12501, doi:10.1029/2009GL038110, 2009.

Fausto, R. S., Mernild, S. H., Hasholt, B., Ahlstrøm, A. P., and Knudsen, N. T.: Modeling suspended sediment concentration and transport, Mittivakkat Glacier, Southeast Greenland, Arctic, *Antarct. Alp. Res.*, 44, 306–318, doi:10.1657/1938-4246-44.3.306, 2012.

Fenn, C. R., Gurnell, A. M., and Beecroft, I. R.: An evaluation of the use of suspended sediment rating curves for the prediction of suspended sediment concentration in a proglacial stream, *Geogr. Ann.*, 67, 71–82, doi:10.2307/520467, 1985.

Goldthwait, R., Mirsky, A., Crowl, G., Koob, D., and Richard, P.: Tasersiaq Area-Sukkertoppen Ice Cap Studies, Report 1701-2, Institute of Polar Studies, The Ohio State University, Columbus, Ohio, 68 pp., available at: <https://kb.osu.edu/dspace/handle/1811/52119>, 1964.

Gregg, W. W. and Casey, N. W.: Sampling biases in MODIS and SeaWiFS ocean chlorophyll data, *Remote Sens. Environ.*, 111, 25–35, doi:10.1016/j.rse.2007.03.008, 2007.

Hanna, E., Huybrechts, P., Steffen, K., Cappelen, J., Huff, R., Shuman, C., Irvine-Fynn, T., Wise, S., and Griffiths, M.: Increased runoff from melt from the Greenland Ice Sheet: a response to global warming, *J. Climate*, 21, 331–341, doi:10.1175/2007JCLI1964.1, 2008.

Harper, J., N. Humphrey, W. T. Pfeffer, J. Brown, and Fettweis, X.: Greenland ice-sheet contribution to sea-level rise buffered by meltwater storage in firn, *Nature*, 491, 240–243, doi:10.1038/nature11566, 2012.

Hasholt, B.: Sediment Transport in Greenland, in *Erosion and Sediment Yield: Global and Regional Perspectives*, IAHS Publ. no. 236, 105–114, available at: http://www.irtces.org/isi/isi_document/iahs236/, 1996.

Hasholt, B., Bobrovitskaya, N., Bogen, J., McNamara, J., Mernild, S. H., Milburn, D., and Walling, D. E.: Sediment transport to the Arctic Ocean and adjoining cold oceans, *Nord. Hydrol.*, 37, 413–432, doi:10.2166/nh.2006.023, 2006.

Hasholt, B., Mikkelsen, A. B., Nielsen, M. H., and Larsen, M. A. D.: Observations of runoff and sediment and dissolved loads from the Greenland Ice Sheet at Kangerlussuaq, West Greenland, 2007 to 2010, *Z. Geomorphol.*, 57, 3–27, doi:10.1127/0372-8854/2012/S-00121, 2013.

Howat, I. M., Negrete, A., Scambos, T., and Haran, T.: A high-resolution elevation model for the Greenland Ice Sheet from combined stereoscopic and photogrammetric data, in preparation, 2013.

MODIS Observed increase in Greenland sediment plumes

B. Hudson et al.

Title Page

Abstract

Introduction

Conclusions

References

Tables

Figures

◀

▶

◀

▶

Back

Close

Full Screen / Esc

Printer-friendly Version

Interactive Discussion



- Hudson, B., Overeem, I., and Syvitski, J. P. M.: A new technique to detect turbid water, and mask clouds in coastal, case two waters, in preparation, 2013.
- Kirk, J. T. O.: Light and Photosynthesis in Aquatic Ecosystems, 3rd edn., Cambridge University Press, Cambridge, UK, 649 pp., 2011.
- 5 Lewis, S. M. and Smith, L. C.: Hydrologic drainage of the Greenland Ice Sheet, *Hydrol. Process.*, 23, 2004–2011, doi:10.1002/hyp.7343, 2009.
- McGrath, D., Steffen, K., Overeem, I., Mernild, S. H., Hasholt, B., and van den Broeke, M.: Sediment plumes as a proxy for local ice-sheet runoff in Kangerlussuaq Fjord, West Greenland, *J. Glaciol.*, 56, 813–821, doi:10.3189/002214310794457227, 2010.
- 10 McGrath, D., Colgan, W., Bayou, N., Muto, A., and Steffen, K.: Recent warming at Summit, Greenland: global context and implications, *Geophys. Res. Lett.*, 40, 1–6, doi:10.1002/grl.50456, 2013.
- Mernild, S. H., Liston, G. E., Steffen, K., and Chylek, P.: Meltwater flux and runoff modeling in the ablation area of Jakobshavn Isbræ, West Greenland, *J. Glaciol.*, 56, 20–32, doi:10.3189/002214310791190794, 2010.
- 15 Mernild, S. H., Liston, G. E., Hiemstra, C. A., Christensen, J. H., Stendel, M., and Hasholt, B.: Surface mass balance and runoff modeling using HIRHAM4 RCM at Kangerlussuaq (Søndre Strømfjord), West Greenland, 1950–2080, *J. Climate*, 24, 609–623, doi:10.1175/2010JCLI3560.1, 2011.
- 20 Miller, R. L. and McKee, B. A.: Using MODIS Terra 250 m imagery to map concentrations of total suspended matter in coastal waters, *Remote Sens. Environ.*, 93, 259–266, doi:10.1016/j.rse.2004.07.012, 2004.
- Mobley, C. D.: Estimation of the remote-sensing reflectance from above-surface measurements, *Appl. Optics*, 38, 7442–7455, 1999.
- 25 Morehead, M. D., Syvitski, J. P. M., Hutton, E. W. H., and Peckham, S. D.: Modeling the temporal variability in the flux of sediment from ungauged river basins, *Global Planet. Change*, 39, 95–110, doi:10.1016/S0921-8181(03)00019-5, 2003.
- Mote, T.: Ablation rate estimates over the Greenland Ice Sheet from microwave radiometric data, *Prof. Geogr.*, 52, 322–331, doi:10.1111/0033-0124.00228, 2000.
- 30 Nghiem, S. V., Hall, D. K., Mote, T. L., Tedesco, M., Albert, M. R., Keegan, K., Shuman, C. A., Di Girolamo, N. E., and Neumann, G.: The extreme melt across the Greenland ice sheet in 2012, *Geophys. Res. Lett.*, 39, L20502, doi:10.1029/2012GL053611, 2012.

MODIS Observed increase in Greenland sediment plumes

B. Hudson et al.

Title Page

Abstract

Introduction

Conclusions

References

Tables

Figures

◀

▶

◀

▶

Back

Close

Full Screen / Esc

Printer-friendly Version

Interactive Discussion

- O'Farrell, C. R., Heimsath, A. M., Lawson, D. E., Jorgensen, L. M., Evenson, E. B., Larson, G., and Denner, J.: Quantifying periglacial erosion: insights on a glacial sediment budget, Matanuska Glacier, Alaska, *Earth Surf. Proc. Land.*, 34, 2008–2022, doi:10.1002/esp.1885, 2009.
- 5 Østrem, G.: Sediment transport in glacial meltwater streams, *Glaciofluvial Glaciolacustrine Sediment*, 23, 101–122, 1975.
- Peckham, S. D.: Geomorphometry in RiverTools, *Dev. Soil Sci.*, 33, 411–430, doi:10.1016/S0166-2481(08)00018-4, 2009.
- Rennermalm, A. K., Smith, L. C., Chu, V. W., Box, J. E., Forster, R. R., Van den Broeke, M. R.,
10 Van As, D., and Moustafa, S. E.: Evidence of meltwater retention within the Greenland ice sheet, *The Cryosphere*, 7, 1433–1445, doi:10.5194/tc-7-1433-2013, 2013.
- Retamal, L., Bonilla, S., and Vincent, W. F.: Optical gradients and phytoplankton production in the Mackenzie River and the coastal Beaufort Sea, *Polar Biol.*, 31, 363–379, doi:10.1007/s00300-007-0365-0, 2008.
- 15 Rignot, E., Box, J. E., Burgess, E., and Hanna, E.: Mass balance of the Greenland ice sheet from 1958 to 2007, *Geophys. Res. Lett.*, 35, L20502, doi:10.1029/2008GL035417, 2008.
- Serreze, M. and Barry, R.: *The Arctic Climate System*, 1st edn., Cambridge Atmospheric and Space Sciences Series, edited by: Houghton, J. T., Rycroft, M. J., and Dessler, A. J., Cambridge University Press, Cambridge, UK, 385 pp., 2005.
- 20 Shepherd, A., Ivins, E. R., A, G., Barletta, V. R., Bentley, M. J., Bettadpur, S., Briggs, K. H., Bromwich, D. H., Forsberg, R., Galin, N., Horwath, M., Jacobs, S., Joughin, I. R., King, M. A., Lenaerts, J. T. M., Li, J., Ligtenberg, S. R. M., Luckman, A., Luthcke, S. B., McMillan, M., Meister, R., Milne, G., Mougnot, J., Muir, A., Nicolas, J. P., Paden, J., Payne, A. J., Pritchard, H., Rignot, E., Rott, H., Sorensen, L. S., Scambos, T. A., Scheuchl, B., Schrama, E. J. O., Smith, B., Sundal, A. V., van Angelen, J. H., van de Berg, W. J., van den Broeke, M. R., Vaughan, D. G., Velicogna, I., Wahr, J., Whitehouse, P. L., Wingham, D. J., Yi, D., Young, D., and Zwally, H. J.: A reconciled estimate of ice-sheet mass balance, *Science*, 338, 1183–1189, doi:10.1126/science.1228102, 2012.
- 25 Satham, P. J., Skidmore, M., and Tranter, M.: Inputs of glacially derived dissolved and colloidal iron to the coastal ocean and implications for primary productivity, *Global Biogeochem. Cy.*, 22, 1–11, doi:10.1029/2007GB003106, 2008.
- Stott, T. A. and Grove, J. R.: Short-term discharge and suspended sediment fluctuations in the proglacial Skeldal River, north-east Greenland, *Hydrol. Process.*, 15, 407–423, 2001.

**MODIS Observed
increase in
Greenland sediment
plumes**

B. Hudson et al.

[Title Page](#)[Abstract](#)[Introduction](#)[Conclusions](#)[References](#)[Tables](#)[Figures](#)[⏪](#)[⏩](#)[◀](#)[▶](#)[Back](#)[Close](#)[Full Screen / Esc](#)[Printer-friendly Version](#)[Interactive Discussion](#)

- Syvitski, J. P. M., Morehead, M. D., Bahr, D. B., and Mulder, T.: Estimating fluvial sediment transport: the rating parameters, *Water Resour. Res.*, 36, 2747–2760, doi:10.1029/2000WR900133, 2000.
- 5 Tedstone, A. J. and Arnold, N. S.: Automated remote sensing of sediment plumes for identification of runoff from the Greenland ice sheet, *J. Glaciol.*, 58, 699–712, doi:10.3189/2012JoG11J204, 2012.
- Toller, G. N., Isaacman, A., Kuyper, J., and Geng, X.: MODIS Level 1B Product User's Guide, NASA, Greenbelt, MD, 57 pp., 2009.
- 10 van den Broeke, M., Bamber, J. L., Ettema, J., Rignot, E., Schrama, E., van de Berg, W. J., van Meijgaard, E., Velicogna, I., and Wouters, B.: Partitioning Recent Greenland Mass Loss, *Science*, 326, 984–986, doi:10.1126/science.1178176, 2009.
- van de Wal, R. S. W., Boot, W., Smeets, C. J. P. P., Snellen, H., van den Broeke, M. R., and Oerlemans, J.: Twenty-one years of mass balance observations along the K-transect, West Greenland, *Earth Syst. Sci. Data*, 4, 31–35, doi:10.5194/essd-4-31-2012, 2012.
- 15 Weidick, A. and Citterio, M.: The ice-dammed lake Isvand, West Greenland, has lost its water, *J. Glaciol.*, 57, 186–188, 2011.

MODIS Observed increase in Greenland sediment plumes

B. Hudson et al.

Title Page

Abstract

Introduction

Conclusions

References

Tables

Figures

⏪

⏩

◀

▶

Back

Close

Full Screen / Esc

Printer-friendly Version

Interactive Discussion

Table 1. Various measures of Greenland Ice Sheet catchments in paper.

| Catchment | Maximum elevation (m) | Minimum elevation (m) | Area (km ²) | Area under ELA (km ²) | Area under ELA (%) | Area-weighted average elevation (m) |
|-----------------------|-----------------------|-----------------------|-------------------------|-----------------------------------|--------------------|-------------------------------------|
| Pakitsuup North | 1169 | 98 | 302 | 300 | 99.3 | 852 |
| Pakitsuup South | 1020 | 84 | 143 | 143 | 100 | 610 |
| Watson | 1860 | 106 | 3640 | 2864 | 79 | 1248 |
| Umiiivit | 2387 | 257 | 6320 | 2072 | 33 | 1734 |
| Sarfartoq | 2157 | 671 | 5385 | 3291 | 61 | 1503 |
| Sarfartoq – GrIS only | 2157 | 728 | 4466 | 2616 | 59 | 1529 |
| Naujat Kuat | 1342 | 228 | 460 | 460 | 100 | 1032 |
| Naujat Kuat – Small | 1342 | 185 | 356 | 356 | 100 | 1049 |

MODIS Observed increase in Greenland sediment plumes

B. Hudson et al.

Table 2. Surface water samples used in retrieval algorithm.

| River plume | Coordinates of river mouth | Dates samples collected | Number of samples used |
|-----------------|-------------------------------|---|------------------------|
| Pakitsuup South | 69°26′5.93″ N, 50°27′53.35″ W | 14 Jul 2011 | 7 |
| Orpigsoq Fjord | 68°38′30.87″ N, 50°54′45.5″ W | 02 Jul 2011 | 3 |
| Watson | 66°57′53.7″ N, 50°51′49.8″ W | 04 Jun 2008, 16 Jun 2010, 09 Jul 2011, 19 Jul 2012, 21 Jul 2012, 23 Jul 2012, 24 Jul 2012 | 74 |
| Umiviit | 66°50′01.6″ N, 50°48′37.3″ W | 23 Jul 2012 | 7 |
| Sarfartoq | 66°29′29.6″ N, 52°1′29.5″ W | 24 Jul 2012 | 5 |
| Naujat Kuat | 64°12′37.5″ N, 50°12′31.0″ W | 30 Jun 2011, 15 Aug 2012, 16 Aug 2012 | 47 |

Title Page

Abstract

Introduction

Conclusions

References

Tables

Figures

◀

▶

◀

▶

Back

Close

Full Screen / Esc

Printer-friendly Version

Interactive Discussion

MODIS Observed increase in Greenland sediment plumes

B. Hudson et al.

Title Page

Abstract

Introduction

Conclusions

References

Tables

Figures

⏪

⏩

◀

▶

Back

Close

Full Screen / Esc

Printer-friendly Version

Interactive Discussion

Table 3. Melt-season mean suspended sediment concentration (SSC_{msm}) percent of 13 yr mean. Underlined values are statistically below the mean, bold values statistically above.

| Year | Pakitsuup Fjord | | Kangerlussuaq Fjord | | | Ameralik Fjord |
|------|-----------------|------------|---------------------|------------|------------|----------------|
| | North | South | Watson | Umiiviit | Sarfartoq | Naujat Kuat |
| 2000 | 85 | 103 | <u>80</u> | 100 | <u>60</u> | 102 |
| 2001 | 101 | <u>79</u> | <u>87</u> | <u>83</u> | <u>77</u> | 111 |
| 2002 | 106 | <u>98</u> | <u>72</u> | 107 | <u>82</u> | 98 |
| 2003 | <u>80</u> | 98 | 126 | 104 | <u>97</u> | <u>79</u> |
| 2004 | <u>93</u> | 96 | 112 | 107 | 100 | <u>79</u> |
| 2005 | 133 | 151 | 108 | 123 | <u>77</u> | 104 |
| 2006 | 134 | 116 | 104 | <u>74</u> | 94 | 102 |
| 2007 | 116 | 142 | 136 | 123 | 125 | 125 |
| 2008 | <u>82</u> | <u>82</u> | 109 | <u>84</u> | 116 | 101 |
| 2009 | 97 | <u>63</u> | <u>82</u> | <u>77</u> | <u>62</u> | <u>71</u> |
| 2010 | 90 | 84 | 129 | 130 | 153 | 133 |
| 2011 | 134 | 116 | <u>80</u> | <u>63</u> | 94 | 94 |
| 2012 | <u>74</u> | 85 | 88 | 143 | 134 | 107 |

MODIS Observed increase in Greenland sediment plumes

B. Hudson et al.

Title Page

Abstract

Introduction

Conclusions

References

Tables

Figures

⏪

⏩

◀

▶

Back

Close

Full Screen / Esc

Printer-friendly Version

Interactive Discussion

Table 4. Percent available fjord pixels in a melt season above 50 mgL^{-1} ($P_{>50}$) as a percent of statistics' 13 yr mean. Underlined values are statistically below the mean, bold values statistically above.

| Year | Pakitsuup Fjord | | Kangerlussuaq Fjord | | | Ameralik Fjord |
|------|-----------------|------------|---------------------|------------|------------|----------------|
| | North | South | Watson | Umiiviit | Sarfartoq | Naujat Kuat |
| 2000 | <u>46</u> | <u>57</u> | <u>60</u> | <u>70</u> | <u>48</u> | <u>68</u> |
| 2001 | <u>83</u> | <u>78</u> | <u>77</u> | <u>73</u> | <u>73</u> | <u>87</u> |
| 2002 | <u>72</u> | <u>69</u> | <u>68</u> | <u>82</u> | <u>65</u> | <u>102</u> |
| 2003 | <u>97</u> | 115 | 132 | 119 | 100 | 103 |
| 2004 | 112 | 121 | 98 | 99 | <u>78</u> | 96 |
| 2005 | <u>88</u> | <u>131</u> | <u>75</u> | <u>74</u> | <u>58</u> | <u>70</u> |
| 2006 | <u>87</u> | <u>60</u> | <u>57</u> | <u>43</u> | <u>54</u> | <u>64</u> |
| 2007 | 112 | 122 | 100 | 100 | 122 | 95 |
| 2008 | 102 | 107 | 119 | 102 | 151 | 129 |
| 2009 | 143 | 93 | 129 | 159 | 97 | 100 |
| 2010 | 109 | 107 | 148 | 122 | 160 | 152 |
| 2011 | 146 | 129 | 103 | <u>88</u> | 119 | <u>84</u> |
| 2012 | 104 | 110 | 134 | 171 | 173 | 151 |

MODIS Observed increase in Greenland sediment plumes

B. Hudson et al.

[Title Page](#)[Abstract](#)[Introduction](#)[Conclusions](#)[References](#)[Tables](#)[Figures](#)[⏪](#)[⏩](#)[◀](#)[▶](#)[Back](#)[Close](#)[Full Screen / Esc](#)[Printer-friendly Version](#)[Interactive Discussion](#)

Table 5. Percent available fjord pixels in a melt season above 250 mgL^{-1} ($P_{>250}$) as a percent of statistics' 13 yr mean. Underlined values are statistically below the mean, bold values statistically above.

| Year | Pakitsuup Fjord | | Kangerlussuaq Fjord | | | Ameralik Fjord |
|------|-----------------|------------|---------------------|------------|------------|----------------|
| | North | South | Watson | Umiiviit | Sarfartoq | Naujat Kuat |
| 2000 | <u>52</u> | <u>87</u> | <u>64</u> | <u>71</u> | <u>40</u> | <u>62</u> |
| 2001 | <u>89</u> | <u>75</u> | <u>83</u> | <u>72</u> | <u>65</u> | <u>97</u> |
| 2002 | <u>83</u> | <u>88</u> | <u>68</u> | <u>89</u> | <u>69</u> | 108 |
| 2003 | <u>83</u> | <u>110</u> | 136 | 124 | <u>101</u> | <u>84</u> |
| 2004 | <u>78</u> | <u>74</u> | 101 | 106 | <u>089</u> | <u>85</u> |
| 2005 | <u>93</u> | 206 | <u>79</u> | <u>85</u> | <u>53</u> | <u>82</u> |
| 2006 | 108 | <u>75</u> | <u>61</u> | <u>39</u> | <u>55</u> | <u>77</u> |
| 2007 | 108 | 150 | 118 | 115 | 122 | 104 |
| 2008 | 92 | 103 | 132 | 109 | 166 | 145 |
| 2009 | 145 | <u>55</u> | 114 | 107 | 57 | <u>69</u> |
| 2010 | 107 | <u>90</u> | 146 | 129 | 176 | 163 |
| 2011 | 171 | 129 | 94 | <u>72</u> | 122 | <u>74</u> |
| 2012 | 91 | <u>59</u> | 104 | 183 | 184 | 151 |

MODIS Observed increase in Greenland sediment plumes

B. Hudson et al.

Title Page

Abstract

Introduction

Conclusions

References

Tables

Figures

◀

▶

◀

▶

Back

Close

Full Screen / Esc

Printer-friendly Version

Interactive Discussion

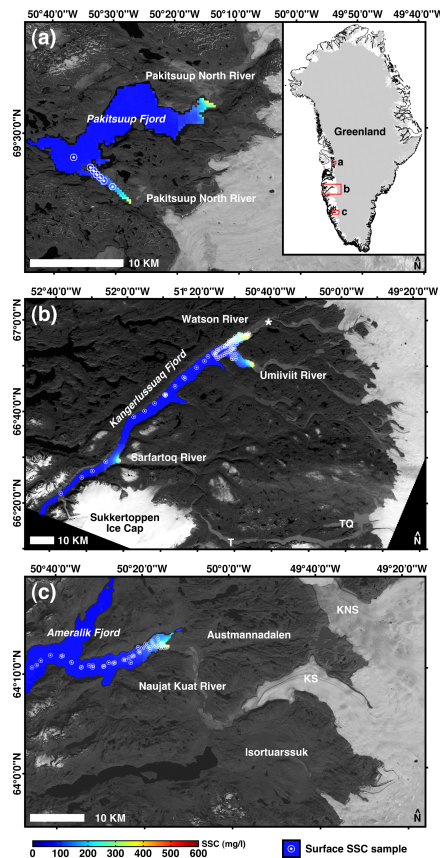


Fig. 1. Overview map of study fjords, with surface suspended sediment concentration (SSC) sample locations used in retrieval overlaid on 13yr mean SSC values derived from MODIS algorithm. Background images are Landsat 7 ETM+ from **(a)** 7 July 2001 **(b)** 20 August 2002, and **(c)** 3 August 2001. Inset shows location of fjords relative to Greenland Ice Sheet. An asterisk shows the location of the Watson River gauge.

MODIS Observed increase in Greenland sediment plumes

B. Hudson et al.

Title Page

Abstract

Introduction

Conclusions

References

Tables

Figures

◀

▶

◀

▶

Back

Close

Full Screen / Esc

Printer-friendly Version

Interactive Discussion

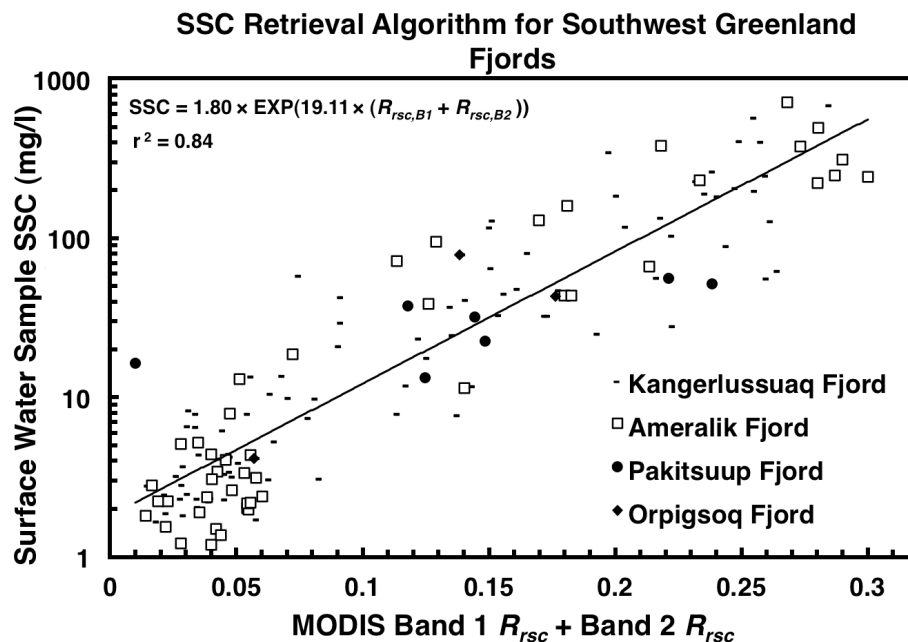


Fig. 2. Relationship between MODIS band one and two corrected remote sensing reflectance (R_{rsc}) and surface water sample SSC values used in retrieval algorithm.

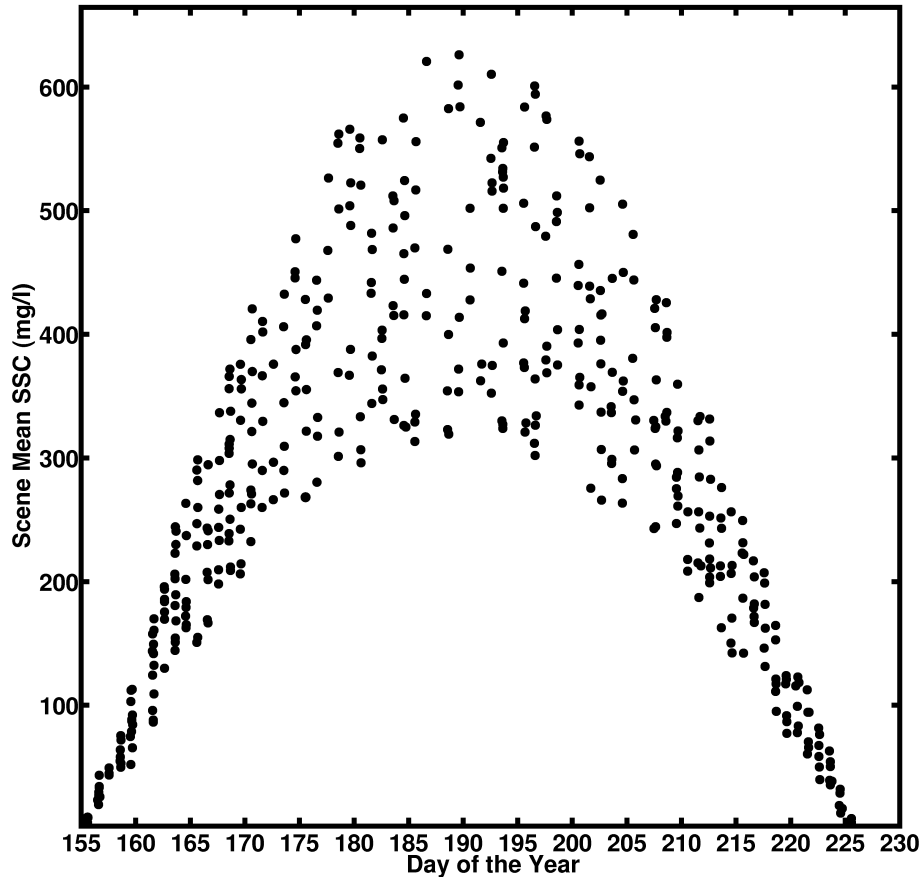


Fig. 3. Example of how “truth” computational experiment allowed scene suspended sediment concentration (SSC) to vary during a simulated melt season. For each scene a scene intensity was randomly generated that controls the scene mean SSC (plotted). Three melt seasons are plotted to show a wider range of SSCs allowed.

**MODIS Observed
increase in
Greenland sediment
plumes**

B. Hudson et al.

| | |
|--------------------------|--------------|
| Title Page | |
| Abstract | Introduction |
| Conclusions | References |
| Tables | Figures |
| ◀ | ▶ |
| ◀ | ▶ |
| Back | Close |
| Full Screen / Esc | |
| Printer-friendly Version | |
| Interactive Discussion | |



MODIS Observed increase in Greenland sediment plumes

B. Hudson et al.

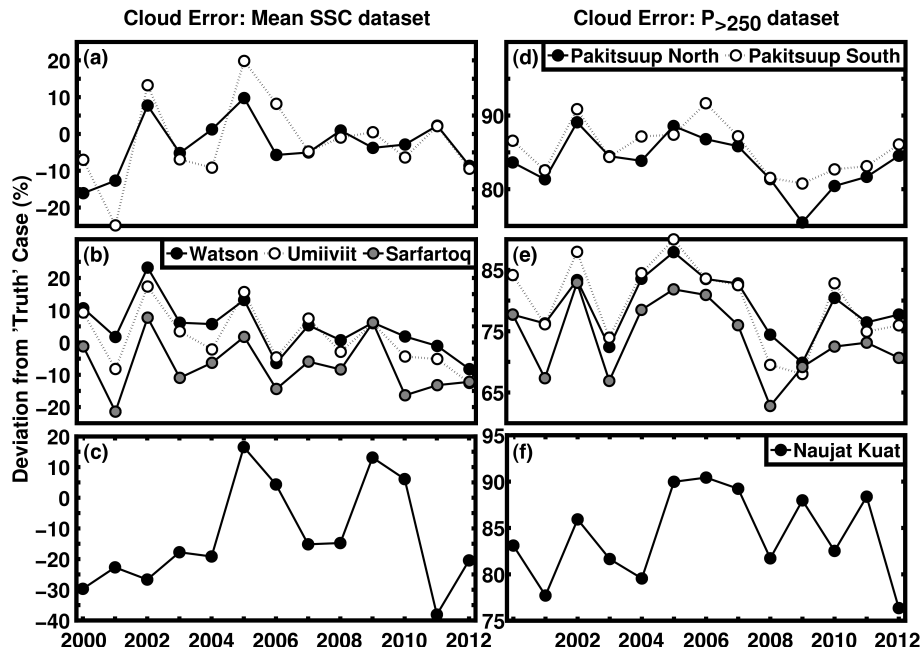


Fig. 5. Deviation of “truth” from MODIS cloud masked “truth” metrics used to constrain error budget. $P_{>50}$ values (not plotted) are similar to $P_{>250}$ values.

| | |
|--------------------------|--------------|
| Title Page | |
| Abstract | Introduction |
| Conclusions | References |
| Tables | Figures |
| ◀ | ▶ |
| ◀ | ▶ |
| Back | Close |
| Full Screen / Esc | |
| Printer-friendly Version | |
| Interactive Discussion | |

MODIS Observed increase in Greenland sediment plumes

B. Hudson et al.

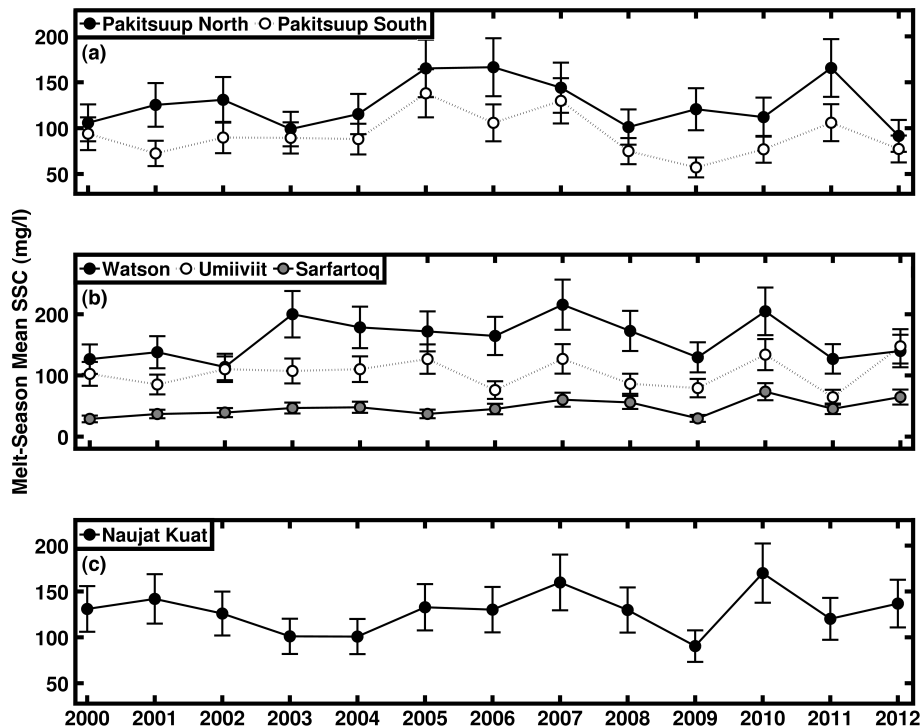
[Title Page](#)
[Abstract](#)
[Introduction](#)
[Conclusions](#)
[References](#)
[Tables](#)
[Figures](#)
[⏪](#)
[⏩](#)
[◀](#)
[▶](#)
[Back](#)
[Close](#)
[Full Screen / Esc](#)
[Printer-friendly Version](#)
[Interactive Discussion](#)


Fig. 6. Melt season mean suspended sediment concentration (SSC_{msm}) for yearly melt season with error bars for **(a)** Pakitsuup, **(b)** Kangerlussuaq, and **(c)** Ameralik fjord plume(s).

MODIS Observed increase in Greenland sediment plumes

B. Hudson et al.

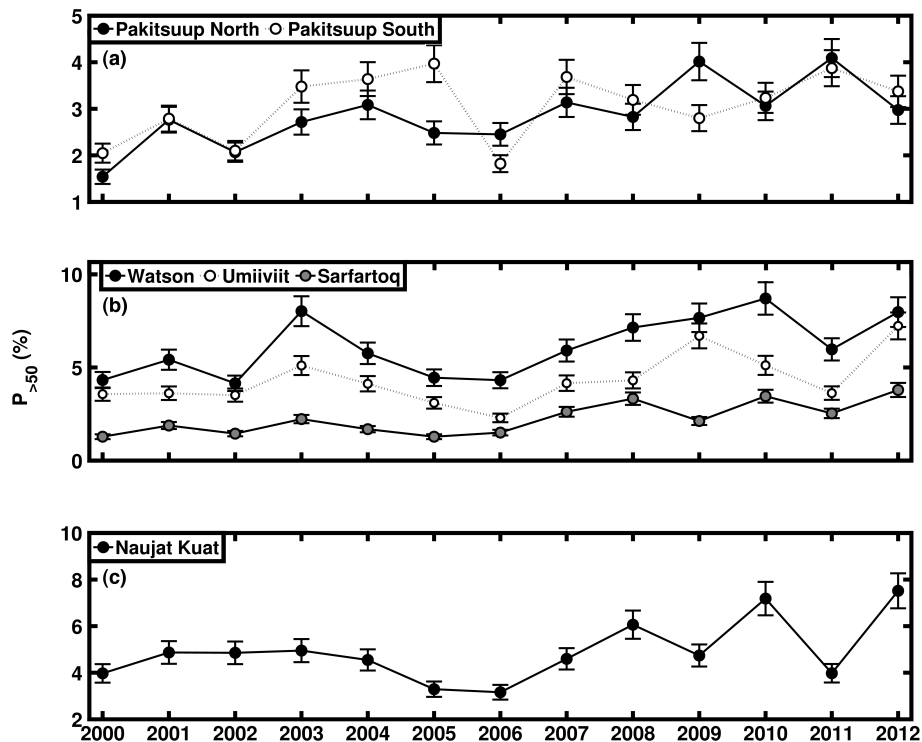


Fig. 7. $P_{>50}$ for yearly melt season with error bars for (a) Pakitsuup, (b) Kangerlussuaq, and (c) Ameralik fjord plume(s).

MODIS Observed increase in Greenland sediment plumes

B. Hudson et al.

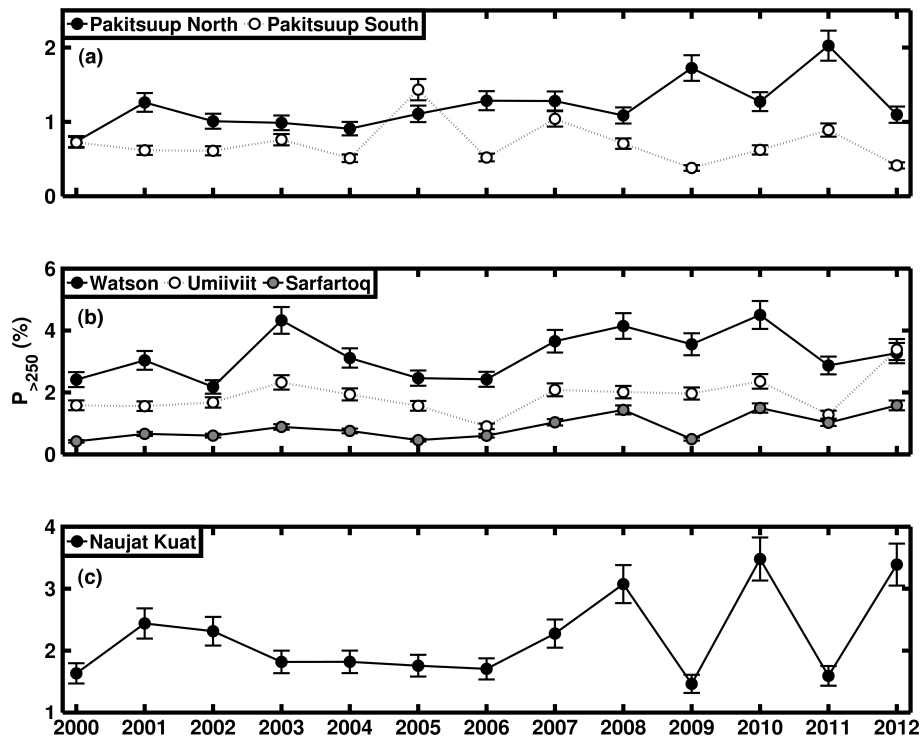


Fig. 8. $P_{>250}$ for yearly melt season with error bars for **(a)** Pakitsuup, **(b)** Kangerlussuaq, and **(c)** Ameralik fjord plume(s).

MODIS Observed increase in Greenland sediment plumes

B. Hudson et al.

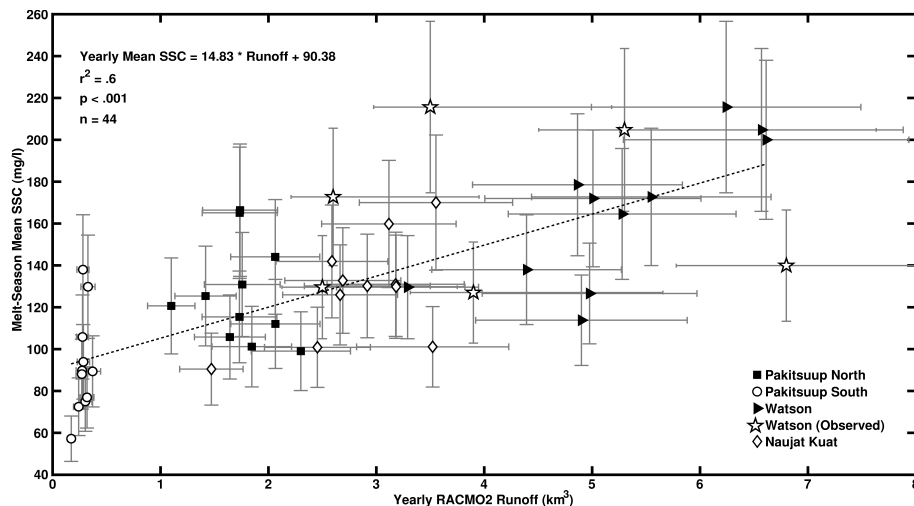


Fig. 9. Relationship between yearly RACMO2 modeled runoff and melt season mean suspended sediment concentration (SSC_{msm}) for four river plumes. Watson River observed discharge and SSC_{msm} plotted for comparison, but these data were not included in relationship.

Title Page

Abstract

Introduction

Conclusions

References

Tables

Figures

⏪

⏩

◀

▶

Back

Close

Full Screen / Esc

Printer-friendly Version

Interactive Discussion

MODIS Observed increase in Greenland sediment plumes

B. Hudson et al.

Title Page

Abstract

Introduction

Conclusions

References

Tables

Figures

◀

▶

◀

▶

Back

Close

Full Screen / Esc

Printer-friendly Version

Interactive Discussion

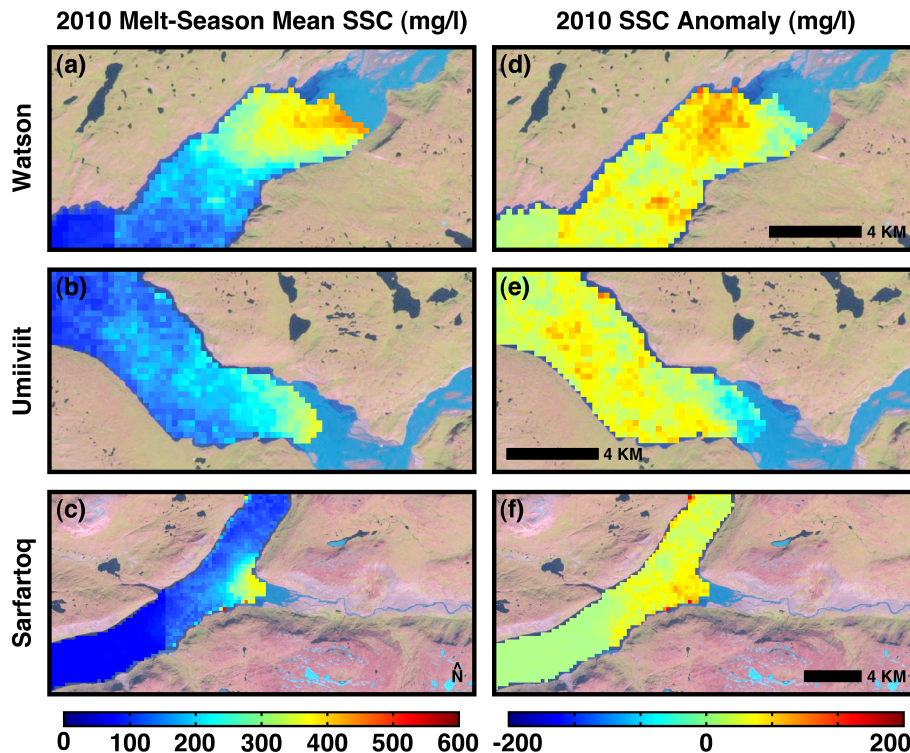


Fig. 10. Maps of 2010 melt season mean suspended sediment concentration (SSC_{msm}) and its anomaly from its 13 yr mean for plume regions of interest. Landsat 7 false color image from 7 July 2001 underlaid for reference.

MODIS Observed increase in Greenland sediment plumes

B. Hudson et al.

Title Page

Abstract

Introduction

Conclusions

References

Tables

Figures

◀

▶

◀

▶

Back

Close

Full Screen / Esc

Printer-friendly Version

Interactive Discussion

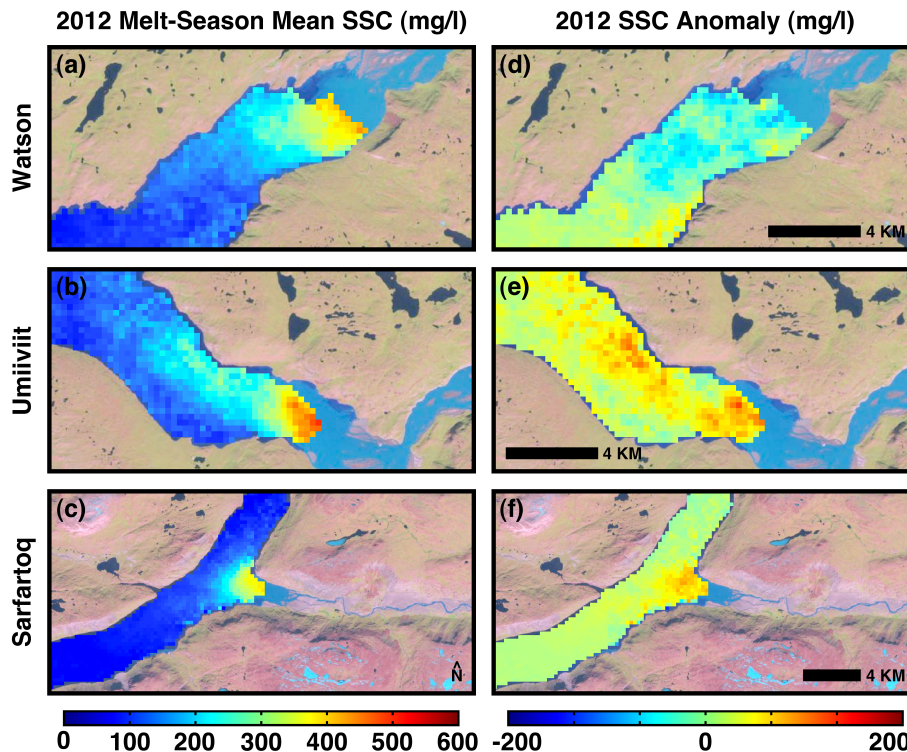


Fig. 11. Maps of 2012 melt season mean suspended sediment concentration (SSC_{msm}) and its anomaly from its 2000 through 2012 mean for plume regions of interest. Landsat 7 false color image from 7 July 2001 underlaid for reference.